Talanta Open 9 (2024) 100297

Contents lists available at ScienceDirect

Talanta Open

journal homepage: www.sciencedirect.com/journal/talanta-open

Radiation evaluation assay using a human three-dimensional oral cancer model for clinical radiation therapy.

Lucie Sercombe [a], Kazuyo Igawa [b,*], Kenji Izumi [c]

[a] Biomedical Engineering Department, Grenoble Institute of Technology, Grenoble 38000, France
[b] Neutron Therapy Research Center, Okayama University, Okayama 700-8558, Japan
[c] Division of Biomimetics, Faculty of Dentistry & Graduate School of Medical and Dental Sciences, Niigata University, Niigata 951-8514, Japan

ARTICLE INFO

Keywords:
Oral cancer model
3D-cell culture
Radiation therapy
Histopathological assay
Radiobiological evaluation

ABSTRACT

With the development of various radiation-based cancer therapies, radiobiological evaluation methods instead of traditional clonogenic assays with monolayer single cell culture are required to bridge gaps in clinical data. Heterogeneity within cancer tissues is the reason for bridging the gap between basic and clinical research in cancer radiotherapy. To solve this problem, we investigated an evaluation assay using a three-dimensional (3D) model of cancer tissue. In this study, a 3D model consisting of tumor and stromal layers was used to compare and verify radiobiological effects with conventional two-dimensional (2D) methods. A significant difference in the response to radiation was observed between the 2D and 3D models. The relative number of cancer cells decreased with X-ray dose escalations in the 2D and 3D models. In contrast, the relative number of normal cells was quite different between the 2D and 3D models. Considering the ability of cells to recover from radiation-induced damage, the histological results of the 3D model were reflected in the clinical data. Histopathological analysis using a 3D model is a potential method for evaluating radiobiological effects on the tumor and tumor margins.

1. Introduction

Cancer is a highly heterogeneous tissue, and the tumor microenvironment (TME) is complex and dynamic. Both cellular components, such as tumor cells and fibroblasts, and non-cellular components, such as the extracellular matrix (ECM), play important roles in tumor development, progression, and outcome of cancer treatment. Therefore, techniques for developing a three-dimensional (3D) cancer model consisting of cellular and non-cellular components to bridge the gap between conventional two-dimensional (2D) monolayer cell culture and animal models have emerged [1]. Compared with 2D, 3D cultures models allow for efficient and relatively easy drug safety and efficacy testing and are known to provide better data regarding the prediction of drug resistance [2] . In addition, compared with 2D and 3D cell culture models, these models can reflect factors that influence radiosensitivity, such as repair, oxygenation, and reoxygenation [3]. In recent years, the research and development of evaluation methods to replace animal experiments in the development of pharmaceuticals and medical devices has been required [4]. Verification of therapeutic effects using 3D culture models with metabolism, anatomy, and pharmacokinetics closer to those of humans is important because it can shorten the development period of medical devices and pharmaceuticals and is expected to have high predictability in human clinical trials [5].

Oral cancer patients are generally treated with surgery for early-stage cancers and with multidisciplinary therapy combining chemotherapy and radiotherapy in addition to surgery for advanced cancers [6]. After cancer treatment, defects may occur in areas where the cancer has died, resulting in ulceration or necrosis of the tissue surrounding the cancer. When the cancer has progressed deep into the oral skin, the dermis is missing and fibroblasts produce collagen to supply the dermal tissue, which covers the oral skin surface. However, if the damage to the surrounding fibroblasts is significant, healing of the oral skin damage is difficult, and skin grafting is necessary. Therefore, it is important to minimize damage to the fibroblasts surrounding the cancer during cancer treatment. Recently, radiation therapy for cancer has enabled the development of devices that generate various types of radiation, such as

Abbreviations: α, linear term of the linear-quadratic model of clonogenic survival; β, quadratic term of the linear-quadratic model of clonogenic survival; 2D, two-dimensional; 3D, Three- dimensional; HSC-4, human tongue squamous carcinoma; NHDF, normal human dermal fibroblasts; LQ model, linear-quadratic model; RBE, relative biological effectiveness; TME, tumor microenvironment.

* Corresponding author at: Neutron Therapy Research Center, Okayama University, Okayama, Japan, 2-5-1 Shikata-cho, Kita-ku, Okayama 700–8558.
E-mail address: igawakazuyo@okayama-u.ac.jp (K. Igawa).

https://doi.org/10.1016/j.talo.2024.100297
Received 16 November 2023; Received in revised form 9 February 2024; Accepted 10 February 2024
Available online 16 February 2024
2666-8319/© 2024 The Authors. Published by Elsevier B.V. This is an open access article under the CC BY-NC-ND license (http://creativecommons.org/licenses/by-nc-nd/4.0/).

X-rays, proton beams, heavy particle beams, and neutron beams, as well as radiation irradiation methods to reduce the radiation dose to surrounding normal tissues, making high precision radiotherapy possible [7]. Although there are many simulation evaluation models for radiotherapy for head and neck cancer, the lack of appropriate clinical predictive models is a challenge for radiotherapy. It is difficult to translate animal models into clinical practice because it is not possible to determine whether an eating disorder is a side effect of treatment. In this study, we developed 3D oral cancer models reflecting TME using squamous carcinoma cells and fibroblasts as cellular components and type-1 collagen as non-cellular components and histologically evaluated oral cancer with surrounding tissue after radiation therapy.

2. Materials and methods

2.1. Human 2D cell culture

Human tongue squamous carcinoma (HSC-4, TIMS (JCRB) Bank, JCRB0624) and normal human dermal fibroblasts (NHDF-Neo, Lot.0000251354; Lonza, Basel, Switzerland),) were used for cell culture. HSC-4 cells were grown in Eagle's minimum essential medium (MEM, Gibco) supplemented with 10% heat-inactivated fetal bovine serum (FBS) and 1% penicillin solution in a humified incubator at 37 °C and 5% CO_2. NHDFs were grown in fibroblast medium-phenol red free (FM-prf, ScienCell) supplemented with 2% FBS (ScienCell), 1% Fibroblast Growth Supplement (FGS, ScienCell), and 1% Penicillin solution (P/S, ScienCell) under the same conditions as those used for HSC-4 cells. The medium was changed every 2 or 3 days. HSC-4 cells and NHDFs were seeded in 6-well plates at a density of 1×10^4 cells per well and cultured for three days.

2.2. Fabrication of a human 3D oral cancer model using HSC-4 and NHDFs

For fabrication of the 3D oral cancer model, the three elements composing the collagen gel matrix were prepared in specific proportions, such as 2800 μL of 0.3% Cellmatrix Type I-A, 800 μL of 5xDME agent and 400 μL Cellmatrix (Nitta gelatin, Osaka, Japan) . The 6-well Thincert plates (Greiner Bio-one, Austria) in which each well had a ThinCerts TC insert with a transparent PET membrane with 3.0 μm pores (Greiner Bio-one, Austria).

On day 0, 1 mL of collagen gel matrix was deposited in each well and incubated for 20 min at room temperature. NHDFs ($5 \times 10\ 5$ cells) with 3 mL of collagen gel matrix were seeded on the acellular collagen gel matrix and incubated for 30 min at 37 °C. This developed a stromal layer in the model. Next, 20 and 2 mL of media were added to the ThinCerts and TC inserts, respectively. On day 2, the stromal layer detached from the insert wall. The stromal layer was then cultured under submerged culture conditions until day 7 with refreshing medium every 2 days. On day 7, after the medium was aspirated, HSC-4 (5×10^5 cells) resuspended in 50 μL of medium were seeded on top of the stromal layer, resulting in the fabrication of a human 3D oral cancer model. This 3D model was incubated under submerged culture conditions for another 7 days, until Day 14 [8]. The complete 3D model is the size of an oval pyramid with a base area of 9.5 square centimeters and a height of approximately 1 cm.

2.3. Radiation treatment

The treatment applied was X-ray radiation on 2D and 3D cultures using an X-ray desktop-operated machine (MX80-Labo Control, medi-Xtec Japan Corporation at 80 kV and 1.25 mA). The radiation doses were 0, 5, 10, and 20 Gy (Fig. 1a). After irradiation, 2D and 3D cultures were cultured for another 5 days (Fig. 1b). The 3D models were cultured at the air–liquid interface with 18 mL of medium in each well, with no medium above the HSC-4 cells. All experiments were conducted in at least triplicate.

2.4. Cell viability assay

In the 2D cell culture, three wells for each radiation level (0, 5, 10 and 20 Gy) were used for counting. On the fifth post-irradiation day in 2D culture, cells were washed twice with PBS and detached with a detaching agent. The detaching agent was TrypLE Express with EDTA without Phenol Red (Gibco, Japan) for NHDFs and 0.5 g/l-Trypsin/0.53 mmol/l-EDTA Solution with Phenol Red (Nacalai Tesque, Japan) for HSC-4 cells. Dead cells were excluded by staining with Trypan Blue 0.4% (Invitrogen, USA), and only live cells were counted using the Automated Cell Counter (Countess II FL, Invitrogen, USA). The survival rate of the cells was defined as the number of live cells treated with radiation divided by the number of live cells that were not treated[9]. Cells inside the 6-well plates were photographed using an inverse microscope

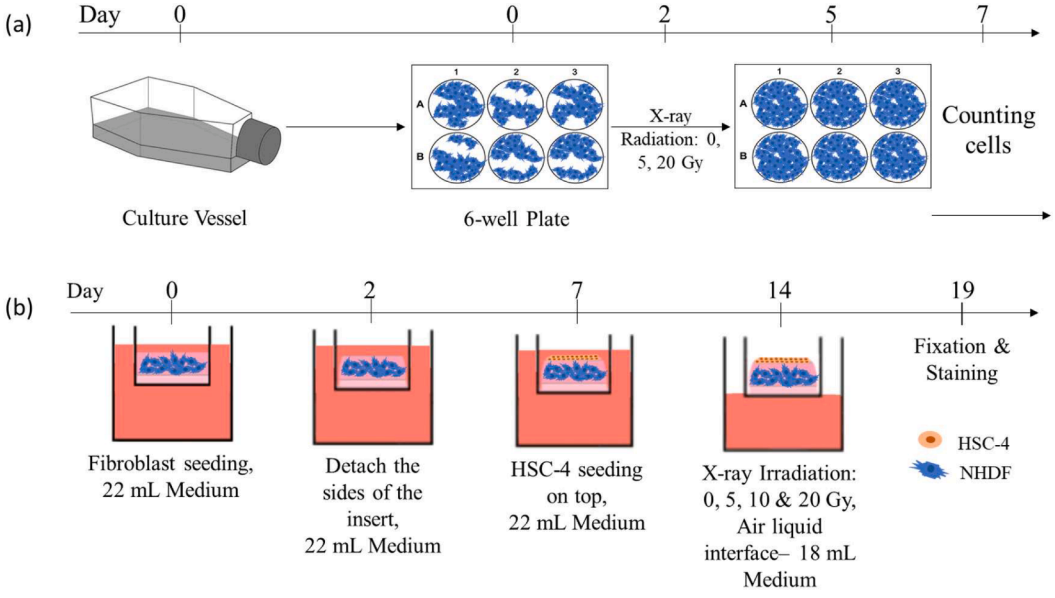

Fig. 1. Protocol of cell culture: (a) Process of 2D cell culture with X-ray irradiation; (b) Process of 3D cell culture with X-ray irradiation.

(DMi1;Leica, Japan).

2.5. Histological analysis

Fixation and staining of the 3D culture model were performed 5 days after irradiation. 3D models were washed twice with D-PBS and fixed in 4% paraformaldehyde phosphate-buffered saline (Fujifilm, Japan) for at least 2 h. The 3D models were dehydrated and embedded in paraffin. Each slice was then cut into very thin transversal slices (5 μm) and stained with Masson's trichrome (MT). Each MT-stained slice was photographed using a BZ-X800 microscope (Keyence, Osaka, Japan). For each dose of radiation, three MT-stained slices were photographed once at a magnification of 10, three times at a magnification (X20), and once at a magnification of 40. The blue-stained collagen-dominant area was defined as the stromal layer, and the purple-red-stained cytoplasmic layer in the upper portion of the stromal layer was designated as the cancer cell layer. The number of cancer cell layers was counted using magnification images (x40) in three different hot spots. A hot spot was defined as an area in which the density of fibroblasts was highest. The stromal and tumor area ratio were measured using ImageJ software (National Institute of Health, USA). The number and size of cancer cells and fibroblasts were measured using ImageJ software. The number of cancer cells was counted using three hot spots in each (x20) magnification image. A hot spot was defined as an area in which the density of cancer cells was highest. The relative number of cells was defined as the number of cells treated with radiation divided by the number of cells that were not treated, which indicates the reduction tendency of number of cells by X-ray irradiation. The number and size of fibroblasts were determined using the magnification images (x10), with the use of ImageJ [10].

2.6. Correlation in 2D and 3 D models

Correlation in HSC-4 cells occupancy was calculated between the 2D and 3 D models. For the 2D data, the survival rate of the cells was calculated as the number of live and dead cells. For the 3D data, the relative number of cells was calculated as the number of cells treated with radiation divided by the number of cells that were not treated. Each relative number of cells had 3 points for each level of radiation (0, 5, 10 and 20 Gy) and these points were matched to each other. The linear regression between both relative number of cells survival rates was calculated using the linear regression model in Python.

2.7. Calculation of the linear–quadratic model

The linear-quadratic (LQ) model was calculated such that the number of surviving cells could be expressed as follows:

$$S = e^{\wedge}\left(-\alpha D - \beta D^2\right), \quad (1)$$

where S is the survival fraction of cells, D is the radiation dose and α and β constants. This expression is the most common way to define the linear–quadratic model [11]. The constants α and β were calculated such that the curve found had the best fit.

2.8. Statistics analysis

The data are shown as three points representing the three values obtained or as means ± standard deviation. Data comparison was performed using multiple unpaired *t*-tests. P-values <0.05, <0.01 were considered statistically significant. All cell experiments were performed in triplicate.

3. Results

3.1. Cell viability of 2D culture after X-ray irradiation

Cell viability in 2D culture evaluated by trypan blue exclusion assay showed a significant decrease in live cell numbers after X-ray irradiation with dose escalation for both cell types (Fig. 2a, 2b). NHDFs were less radiosensitive to X-ray irradiation than HSC-4, with 3% NHDF survival at 20 Gy and 1% HSC-4 survival at 20 Gy (Fig 2c, 2d).

3.2. Effect of 3D culture after X-ray irradiation

The number of cancer layers and the tumor area significantly decreased in an X-ray irradiation dose dependent manner (Fig. 3a, b). The stromal area follows an inverse trend to the tumor area with dose escalation. The size of the cancer cells increased as the irradiation dose increased, doubling with 20 Gy irradiation compared with 0 Gy ($p<0.01$). In contrast, the overall size of the NHDFs followed the same trend (Fig. 4a,b). The relative number of cells in 3D culture evaluated by histological assay showed that the sensitivity of NHDFs to X-ray irradiation was decreased (Fig. 4c). HSC-4 cells were more sensitive to X-ray radiation, with 30% relative cell numbers after X-ray irradiation at 20 Gy (Fig. 4d). HSC-4 cells had the same radiosensitivity to both doses of 10 and 20 Gy.

3.3. Correlation of cell occupancy in 2D and 3D models

The HSC-4 cell occupancy rate showed a correlation ($R = 0.94$) between 2D and 3D cell cultures; however, 2D cell cultures had a higher radiosensitivity to X-ray radiation than 3D cell cultures (Fig. 5). For the same dose, the cancer cell occupancy of the 2D cell culture will be lower than that of the 3D cell culture. The NHDF cell occupancy rate in the 2D and 3D models did not correlate.

3.4. Linear– quadratic model of 2D and 3D cell cultures

For better comparability, the coefficients alpha and beta of the survival curve were calculated (Table 1). HSC-4 showed higher values corresponding to higher radiosensitivity compared with NHDFs in both 2D and 3D cell cultures.

4. Discussion

Particle therapy, a type of radiotherapy, has attracted attention because of its properties that make it suitable for cancer treatment in terms of both dose concentration and biological effects. The relative biological effectiveness (RBE) is used as an indicator to show that the intensity of biological effects varies with the type of radiation. Because the cell-killing effect of X-ray therapy is 1, the RBE value of proton therapy is 1.1–1.2 and that of carbon beam therapy is 2–3 [12]. That is, higher RBE values indicate higher cell-killing ability, which means that particle beams are more effective in cancer treatment than X-rays [13]. However, because it is important that particle therapy also has no damage to normal tissues, a high RBE to normal tissues surrounding the tumor is not applied for particle therapy because the damage to normal tissues is also high. On the other hand, the RBE value is calculated by performing cell irradiation experiments with dose escalation and fitting the LQ model to the cell viability using the colony assay method [14]. For the cell irradiation assay, human or animal cell lines are used, and there is a gap with human clinical trials and simulations [15] . While the colony assay is an effective method in tumor cells, it is difficult to quantify the biological effects of radiation in normal cells because normal cells usually do not form colonies regardless of irradiation [16]. To investigate a more clinically relevant method of quantifying biological effects, we developed a 3D model consisting of human normal and cancer cells to evaluate radiation treatment. In this study, the

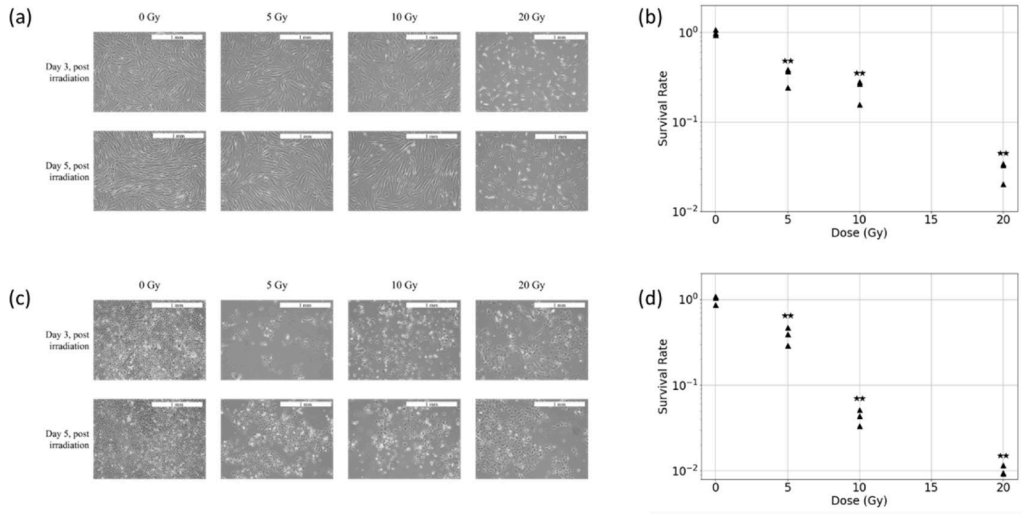

Fig. 2. Cell viability assays after irradiation of 2D culture: (a) NHDF morphology after X-ray irradiation under a microscope (X); (b) survival rate of NHDF after X-ray irradiation (**$p<0.01$); (c) HSC-4 morphology after X-ray irradiation under a microscope (X); (d) survival rate of HSC-4 after X-ray irradiation (**$p<0.01$).

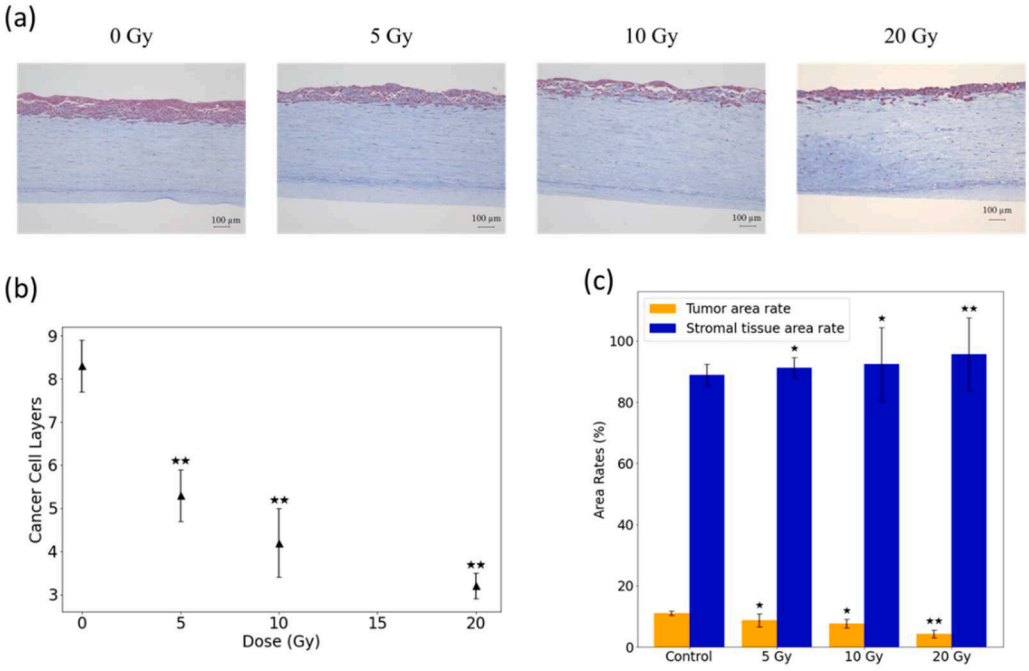

Fig. 3. Effect of different doses of X-ray irradiation on 3D cell culture at 5 days after irradiation: (a) Masson's trichrome-stained sections of 3D cell culture; (b)) Number of layers of cancer cells after X-ray irradiation; (c) Area ratio of the tumor and stromal tissue after X-ray irradiation. Data are presented as mean ±SEM (*$p<0.05$; **$p<0.01$).

radiobiological efficacy of both tumor and normal cells in 2D and 3D cultures was evaluated to assess the normal tissue surrounding the tumor region (Figs. 3 and 4). A correlation of tumor cell number rates was observed between 2D and 3D cell cultures (Fig. 5). However, there was no correlation between fibroblast cell number rates in 2D and 3D cell cultures. Because the LQ model has been best validated by experimental and clinical data, the LQ parameters α, β were calculated in the 2D and 3D models (Table 1). In clinical radiotherapy, there is validation of LQ parameters [15],because tumors are highly heterogeneous structures. There have been several reports comparing radiation tumor response between 2D and 3D cell culture models [3], but the tumor radiological response in 2D and 3D models was different in other studies as well as in our results [17]. Considering radio resistance, the evaluation assay using 3D model will assist in clinical radiation therapy studies. In addition, there are many radiobiological simulation models for experimental and clinical studies [18], however the radiobiological parameters in the model are calculated with the clinical 2D monolayer clonogenic assay. Currently, although there are guidelines for the measurement of RBE values to be reflected in radiotherapy planning for physical methods, there are no guidelines for biological methods, partly due to the difficulty of handling cell samples in the field [19]. This simple 3D model, consisting of cancer layers and stroma, can be determined histologically as well as clinically, and thus is useful for evaluating biological effects as a clinical predictive model that reflects the clinical situation. In addition, this 3D oral model is an ideal system for observing histological changes after irradiation because the stroma is in contact with the medium and the tumor site with air, mimicking the tumor microenvironment of head and neck cancer, which interacts with

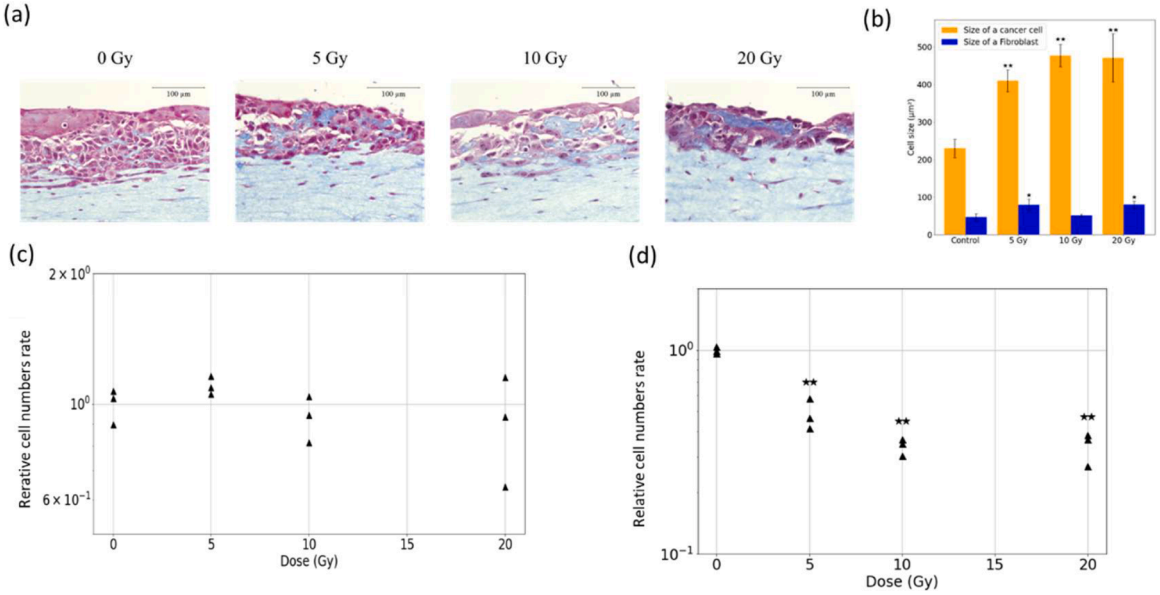

Fig. 4. Histopathological assays after 3D cell culture irradiation: (a) Microscopic image of NHDF and HSC-4 cells after X-ray irradiation; (b) size of cancer cells and fibroblasts after X-ray irradiation; (c) relative number of NHDF cells after X-ray irradiation; (d) relative number of HSC-4 cells after X-ray irradiation (**$p<0.01$).

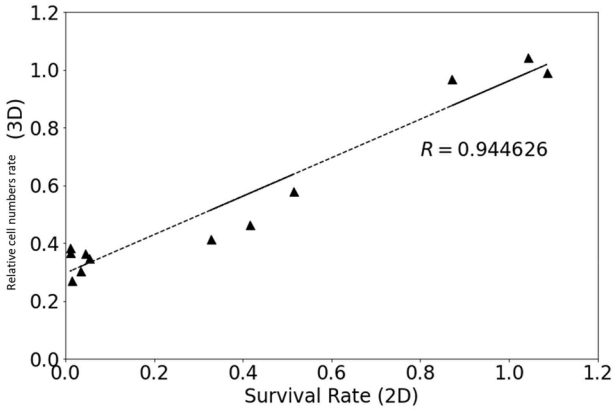

Fig. 5. Correlation between 2D and 3D cell cultures: Correlation between the survival rate of HSC-4 cells in 2D cell culture (abscissa) and the relative cell number rate of HSC-4 cells in 3D cell culture after X-ray irradiation, correlation coefficient $R = 0.944626$.

Table 1
Linear-quadratic model constants α and β for NHDF and HSC-4 in 2D and 3D cell cultures.

	α [Gy^{-1}]	β [Gy^{-1}]
NHDFs (2D)	0.1732587	0.0007473
NHDFs (3D)	−0.0166301	0.00131585
HSC-4 (2D)	0.31995	−0.00413824
HSC-4 (3D)	0.162555	−0.00543156

both liquid and air (Fig. 2b). Considering radio resistance, the 3D model, including our model, will be an evaluation tool for the radiobiological response. In the future, it may be possible to develop a 3D model to directly evaluate biological doses in radiotherapy.

5. Conclusion

We successfully developed a 3D oral cancer model consisting of human oral squamous carcinoma cells and human fibroblasts to investigate the effects of radiation therapy not only on the tumor regions but also on the peritumoral stroma. This 3D model was useful for examining histological changes in and around the tumor region after radiotherapy because biopsy-based examination is not performed after cancer treatment unless the cancer recurrence. The 3D model is a potential clinical prediction tool; however, it needs to be refined as a long-term post-treatment observation model.

Funding

This research was partially supported by JSPS KAKENHI Grant Number JP23K11918.

CRediT authorship contribution statement

Lucie Sercombe: Data curation, Formal analysis, Investigation, Methodology, Software, Validation, Visualization, Writing – original draft. **Kazuyo Igawa:** Conceptualization, Data curation, Funding acquisition, Investigation, Methodology, Project administration, Resources, Supervision, Validation, Visualization, Writing – original draft, Writing – review & editing. **Kenji Izumi:** Resources, Writing – review & editing.

Declaration of competing interest

The authors declare no conflicts of interest.

Data availability

Data will be made available on request.

Acknowledgments

We would like to thank the Institute of Central Research Laboratory, Okayama University Medical School, for assistance with histological analysis and the Advanced Science Research Center, Okayama University, for the use of X-ray irradiation equipment.

References

[1] O.E. Atat, et al., 3D modeling in cancer studies, Hum. Cell 35 (1) (2022) 23–36.

[2] S.A. Langhans, Three-dimensional in vitro cell culture models in drug discovery and drug repositioning, Front. Pharmacol. 9 (2018).
[3] F. Antonelli, 3D cell models in radiobiology: improving the predictive value of in vitro research, Int. J. Mol. Sci. 24 (13) (2023) 10620.
[4] S.M. Badr-Eldin, et al., Three-dimensional in vitro cell culture models for efficient drug discovery: progress so far and future prospects, Pharmaceuticals. (Basel) 15 (8) (2022).
[5] L. Liu, et al., Patient-derived organoid (PDO) platforms to facilitate clinical decision making, J. Transl. Med. 19 (1) (2021) 40.
[6] L.Q.M. Chow, Head and Neck Cancer, New England Journal of Medicine 382 (1) (2020) 60–72.
[7] L. Beaton, et al., How rapid advances in imaging are defining the future of precision radiation oncology, Br. J. Cancer 120 (8) (2019) 779–790.
[8] K. Haga, et al., Crosstalk between oral squamous cell carcinoma cells and cancer-associated fibroblasts via the TGF-β/SOX9 axis in cancer progression, Transl. Oncol. 14 (12) (2021) 101236.
[9] S. Wang, et al., The accelerator-based boron neutron capture reaction evaluation system for head and neck cancer, Appl. Radiat. Isotopes 165 (2020) 109271.
[10] M.N. Gurcan, et al., Histopathological image analysis: a review, IEEe Rev. Biomed. Eng. 2 (2009) 147–171.
[11] S.J. McMahon, The linear quadratic model: usage, interpretation and challenges, Phys. Med. Biol. 64 (1) (2018) 01tr01.
[12] Y. Matsumoto, et al., A critical review of radiation therapy: from particle beam therapy (Proton, Carbon, and BNCT) to beyond, J. Pers. Med. 11 (8) (2021).
[13] K. Sekihara, et al., Evaluation of X-ray and carbon-ion beam irradiation with chemotherapy for the treatment of cervical adenocarcinoma cells in 2D and 3D cultures, Cancer Cell Int. 22 (1) (2022) 391.
[14] S. Mein, et al., How can we consider variable RBE and LET(d) prediction during clinical practice? A pediatric case report at the Normandy Proton Therapy Centre using an independent dose engine, Radiat. Oncol. 17 (1) (2022) 23.
[15] C.M. van Leeuwen, et al., The alfa and beta of tumours: a review of parameters of the linear-quadratic model, derived from clinical radiotherapy studies, Radiat. Oncol. 13 (1) (2018) 96.
[16] P.G.S. Prasanna, et al., Normal tissue protection for improving radiotherapy: where are the Gaps? Transl. Cancer Res. 1 (1) (2012) 35–48.
[17] J. Raitanen, et al., Comparison of radiation response between 2D and 3D cell culture models of different human cancer cell lines, Cells 12 (3) (2023).
[18] B. Jones, R.G. Dale, The evolution of practical radiobiological modelling, Br. J. Radiol. 92 (1093) (2019) 20180097.
[19] C.P. Karger, et al., The RBE in ion beam radiotherapy: in vivo studies and clinical application, Z. Med. Phys. 31 (2) (2021) 105–121.